Journal of Catalysis **209,** 105–113 (2002)
doi:10.1006/jcat.2002.3640

Two Active Sites for Photocatalytic Oxidation of Formic Acid on TiO_2: Effects of H_2O and Temperature

Darrin S. Muggli[1] and Michael J. Backes

Department of Chemical Engineering, University of North Dakota, Grand Forks, North Dakota 58202-7107

Received November 29, 2001; revised April 10, 2002; accepted April 11, 2002

Photocatalytic oxidation (PCO) of formic acid on TiO_2 produces CO_2 without forming any long-lived intermediates. Formic acid PCO is not limited by surface diffusion of either formic acid or active oxygen species. The formic acid oxidation rate increases significantly with temperature up to 373 K, which was the highest temperature used in this study. At least two types of active sites exist for PCO of formic acid on TiO_2 and their activities differ by a factor of at least 20. The more-active sites comprise less than one-fourth of a room-temperature formic acid monolayer. Water, which is produced during PCO, redistributes adsorbed formic acid by displacement. Water readily displaces approximately one-third of a formic acid monolayer but it does not effectively compete for the remaining formic acid adsorption sites. © 2002 Elsevier Science (USA)

INTRODUCTION

Volatile organic compounds (VOCs) are major contributors to air pollution. Many waste streams that contain VOCs are dilute in air with the VOC concentration below 1000 ppm (1–5). For low concentrations, an efficient low-temperature remediation method is preferable to high-temperature catalytic oxidation or thermal incineration. Heterogeneous photocatalytic oxidation (PCO) effectively removes low concentrations of organic contaminants *at room temperature* from both gas and liquid phases by oxidizing organics to environmentally benign compounds (1–16). During PCO, near-UV irradiation of a semiconductor catalyst (usually TiO_2) excites electrons from the valence to the conduction band, leaving holes behind. These electron–hole pairs migrate to the surface where they oxidize adsorbed organics to CO_2 and H_2O.

Transient reaction is a powerful technique for probing the surface processes during photocatalytic oxidation. Transient reaction techniques have been employed to compare activities of different catalysts (17, 18), correlate adsorption sites with PCO behavior (3, 4, 11), determine the role of lattice oxygen during PCO (12–14, 19, 20), identify strongly adsorbed intermediates and determine PCO mechanisms (2, 4, 21–25), and design a photocatalyst with increased selectivity to partial oxidation products (11). These transient studies provided information on the PCO surface processes that would not be easily determined by steady-state reaction.

Although transient reaction techniques have proven to be useful in studying the surface processes during PCO, care must be taken when interpreting transient reaction data. Previous transient PCO studies (4, 12–14, 21, 24) measured high PCO rates for carboxylic acids, indicating that they react readily on TiO_2. In contrast, steady-state studies (26–29) using the same acids found that these species accumulate on the surface, suggesting that they react slowly and may poison the surface. This study analyzes transient PCO of a model carboxylic acid, formic acid, to resolve the differences between transient and steady-state PCO studies. In addition, studying formic acid PCO provides a better understanding of surface processes and adsorption site activity because formic acid oxidizes to CO_2 without forming any long-lived intermediates (1, 4), so that the surface reaction rate can be measured directly. Specifically, this study will show that multiple reaction sites exist for formic acid PCO and formic acid adsorbed at less-active sites is displaced by H_2O to more-active sites during PCO.

EXPERIMENTAL METHODS

The transient and temperature-programmed reaction system used in this study has been described previously (13). An annular Pyrex reactor, which was identical to those used in previous studies (13, 18), allowed for high gas flow rates and uniform UV irradiation of the catalyst. Approximately 30 mg of each catalyst was coated in a thin layer (average thickness <0.4 μm) in the annular region of the reactor. During PCO, 12 UV lamps (Johnlite, 8 W) surrounded the reactor to uniformly irradiate the catalyst. These lamps generate light in the 300 to 500 nm range with a maximum intensity near 360 nm (30). A furnace made of Ni–Cr wire wrapped around a quartz cylinder surrounded the reactor. The end of a 0.5-mm chromel-alumel, shielded

---

[1] To whom correspondence should be addressed. Fax: 701-777-3773. E-mail: darrin_muggli@und.nodak.edu.

thermocouple contacted the catalyst film to provide feedback to the temperature programmer. A Balzers QMS 200 quadrupole mass spectrometer monitored the reactor effluent directly downstream of the reactor. A 25-μm ID fused silica capillary, which fed directly to the mass spectrometer ionizer, sampled the reactor effluent. This sampling system provided high sensitivity and detected gas-phase species rapidly. A computer that was interfaced with the mass spectrometer recorded multiple mass peaks simultaneously. Calibration was performed by injecting known amounts of each species into the gas flow downstream of the reactor. Integration of the areas under the calibration curves provided a means to convert mass spectrometer signals to reaction rates.

Before each isothermal PCO, the reactor was held for 20 min at 723 K in 100 sccm flow of 20% O_2 in He (Praxair, UHP) to create a reproducible surface. For transient PCO at room temperature, three pulses (850 μmol/g catalyst each) of formic acid (Aldrich, 96%) were injected upstream of the reactor so that formic acid adsorbed onto the catalyst. Transient PCO was carried out after the carrier gas flushed excess gas-phase formic acid from the reactor. After a shield was placed between the lights and the reactor, the lights were turned on and allowed to reach a steady output for approximately 10 min. Removing the shields exposed the catalyst to UV irradiation and initiated transient PCO. After transient PCO for a specified time, the UV lights were switched off and either temperature-programmed desorption (TPD) or oxidation (TPO) identified surface species that did not desorb during PCO. TPD was carried out in pure He flow. The Ni–Cr furnace heated the catalyst at 1 K/s to 723 K and maintained this temperature until no products were detected in the gas phase. After cooling the catalyst to room temperature, a subsequent TPO oxidized species that did not desorb during TPD. The TPO procedure was identical to that of TPD, except the carrier gas was 20% O_2 in He.

RESULTS

Transient PCO

Figure 1 (top panel) shows the CO_2 formation rate during transient PCO of a monolayer of formic acid. After UV irradiation of the catalyst at 60 s, oxidation of adsorbed formic acid to CO_2 quickly reached a maximum rate. The CO_2 formation rate decreased slowly during the first 50 s of PCO, after which it decreased more rapidly. Monitoring the CO_2 formation rate is a direct measurement of the surface reaction since CO_2 appearance in the gas phase is reaction limited and not desorption limited. This was shown in several experiments in which the UV lights were turned off after 60–300 s of PCO and the CO_2 formation rate dropped quickly to zero. The immediate maximum in the CO_2 formation rate (Fig. 1, top panel) indicates that formic acid oxidized to CO_2 without forming any long-lived intermediates. After PCO stopped, a subsequent TPD confirmed that only formic acid and H_2O were adsorbed. Formic acid coverage was determined by summing the amounts of CO_2 that formed during PCO with those of CO and CO_2 that desorbed during subsequent TPO. For Degussa P-25 TiO_2, a monolayer of formic acid contained 375 ± 25 μmol/g catalyst, which is in good agreement with the value of 345 reported by Muggli *et al.* (4).

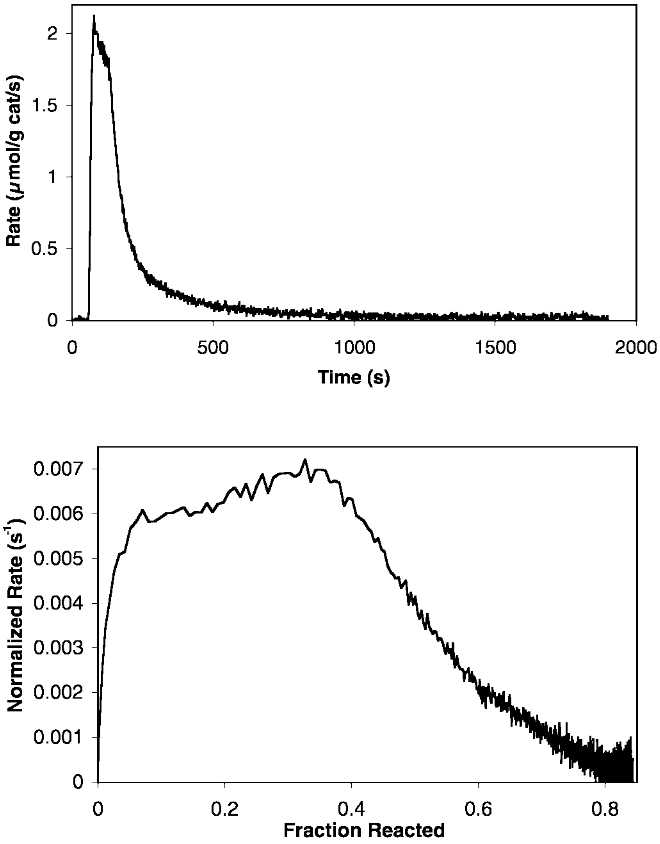

FIG. 1. The CO_2 formation rate (top) and normalized CO_2 formation rate (bottom) during transient PCO of a formic acid monolayer on TiO_2 in 20% O_2 at room temperature. The UV lights were turned on at 60 s and turned off at 1800 s.

The CO_2 formation rate curve in Fig. 1 (top panel) was further analyzed to explore the activities of the formic acid adsorption sites on TiO_2. The CO_2 formation rate was normalized by dividing it by the amount of formic acid that remained adsorbed at each sample point. For example, the CO_2 formation rate after 100 s of PCO was divided by the formic acid coverage at 100 s. Figure 1 (bottom panel) plots this normalized rate versus the fraction of a formic acid monolayer that formed CO_2 to show the change in catalyst activity with formic acid coverage. The plot shows that the normalized CO_2 formation rate increased from an initial value of 6×10^{-3} to a maximum of 7×10^{-3} s^{-1} after 35% of the formic acid monolayer formed CO_2 and then subsequently decreased.

After 80% of a formic acid monolayer oxidized, the normalized CO_2 formation rate remained constant at 4.0×10^{-4} s^{-1}, which is more than an order of magnitude less than the initial catalyst activity. Although the experiment shown in Fig. 1 was stopped after 85% of a formic acid monolayer reacted, other PCOs that were carried out for longer times confirmed that the normalized rate remained constant after 80% of the formic acid monolayer reacted.

PCO with Heating

Several formic acid PCOs were carried out in which the catalyst was heated to temperatures at or below 373 K before or during PCO. TPD of formic acid showed that formic acid does not react without UV at temperatures below 400 K. Therefore, any change in PCO rate after heating TiO_2 to 373 K was not the result of formic acid reacting thermally to form new surface species. To further determine the effect of heating formic acid to 373 K, a monolayer of adsorbed formic acid was heated to 373 K and cooled to room temperature prior to performing PCO. Heating to 373 K desorbed approximately 20% of the formic acid monolayer, and during subsequent PCO (Fig. 2), the initial normalized CO_2 formation rate was the same as a formic acid monolayer. This indicates that heating to 373 K did not cause adsorbed formic acid to react to a species that oxidized more rapidly during PCO. Figure 2 shows that the normalized CO_2 formation rate started to decrease at the same coverage as did PCO of a formic acid monolayer.

Figure 3 shows transient PCOs carried out at temperatures ranging from 298 to 373 K. As temperature increased from 298 to 373 K, the amount of adsorbed formic acid decreased from 375 to 315 μmol/g catalyst, but the maximum CO_2 formation rate doubled. Figure 3 shows that the initial normalized CO_2 formation rate at 373 K was approximately 2.3 times that at room temperature. At all PCO temperatures, the normalized rate started to decrease when formic acid coverage was approximately equal to 65% of a monolayer.

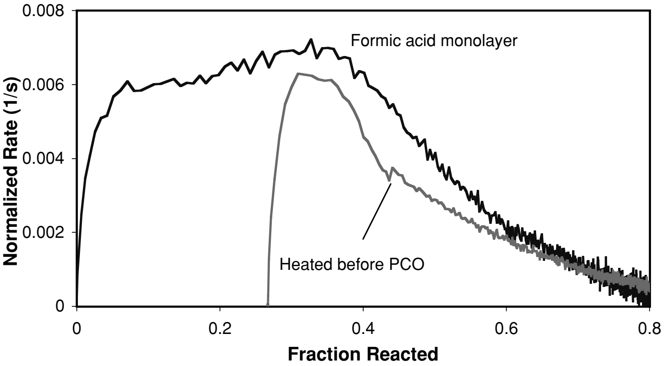

FIG. 2. Normalized CO_2 formation rates during room-temperature transient PCO of formic acid with and without preheating the catalyst to 373 K.

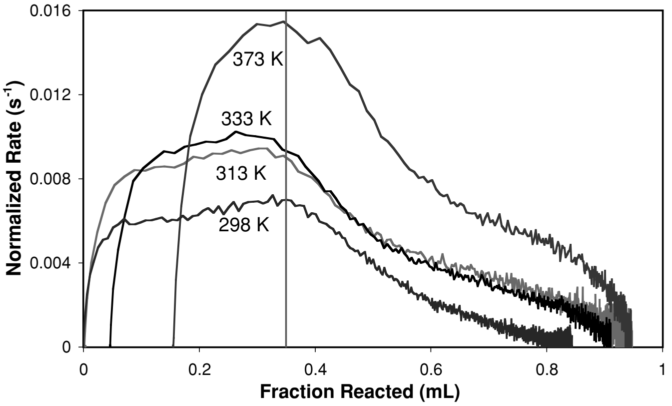

FIG. 3. Normalized CO_2 formation rates during transient PCO of formic acid at various temperatures.

In Figure 4, room-temperature PCO of formic acid was stopped after 130 s of UV irradiation, the catalyst was heated in the dark to 373 K, and PCO was resumed after cooling to room temperature. The mass spectrometer detected H_2O but not formic acid desorption when the catalyst was heated. This contrasts TPD of a formic acid monolayer in which weakly bound formic acid desorbed at 373 K. Since formic acid coverage was less than a monolayer after 130 s of PCO, any weakly bound formic acid that desorbed during heating subsequently readsorbed on vacant catalyst sites. Therefore, heating removed adsorbed H_2O and redistributed formic acid on the surface. When room-temperature PCO resumed after heating and cooling in the dark, catalyst activity more than doubled; the CO_2 formation rate after the dark time was 2.6 times the rate before the lights were turned off. The lights were turned off and the catalyst was heated and cooled in the dark two more times during the experiment; the CO_2 formation rate after PCO resumed was 2.4 and 2.0 times greater than before the lights were turned off for these two subsequent heatings, respectively. Figure 4 shows that after the first heating, the normalized CO_2 formation rate increased to a value that was 10% greater than the previous maximum but it decreased quickly after reaching a maximum, in contrast to the slightly increasing normalized rate initially. The increase in PCO rate after heating (Fig. 4) may be due to either redistribution of formic acid on the surface or removal of H_2O which desorbed during heating. Additional experiments investigated the role of H_2O during PCO.

PCO of Formic Acid and H_2O

Figure 5 shows PCO of formic acid with and without coadsorbed H_2O. Injecting 2 and 8 μL of H_2O displaced 24

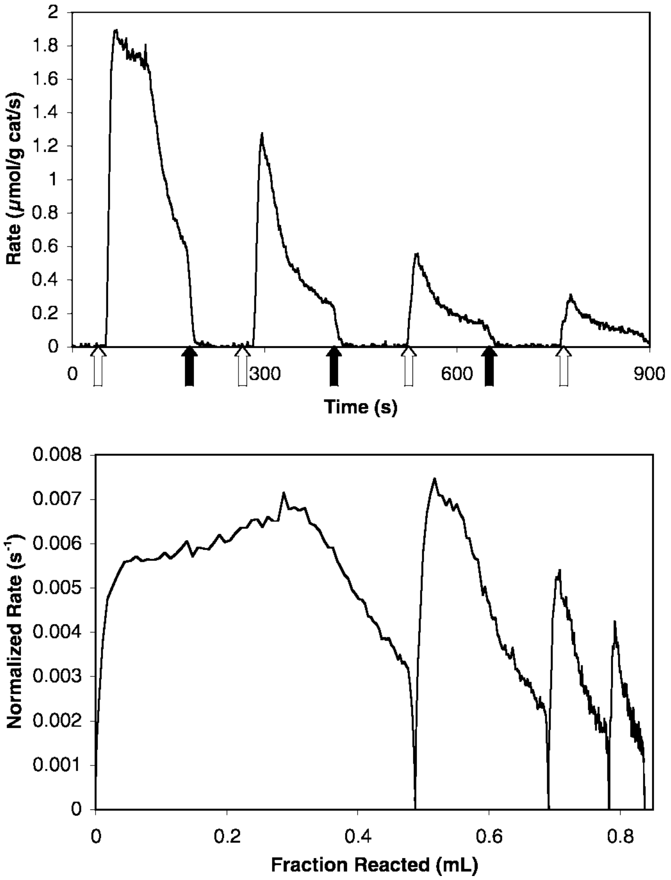

FIG. 4. CO_2 formation rates (top) and normalized CO_2 formation rates (bottom) during transient PCO of formic acid. The lights were turned off (black arrows) and on (white arrows) during the experiment. During the dark periods, the catalyst was heated to 373 K and then cooled to room temperature.

and 30% of the formic acid monolayer, respectively. During subsequent TPOs, the amounts of H_2O that desorbed were 410, 410, and 440 μmol H_2O/g catalyst after PCO of a formic acid monolayer with 0-, 2-, and 8-μL H_2O pulses, respectively. Injecting 2 μL of H_2O decreased formic acid coverage by 90 μmol formic acid/g catalyst but the amount of H_2O that desorbed was the same as a formic acid monolayer. Since one molecule of adsorbed formic acid produces one molecule of H_2O during TPD, the amount of H_2O adsorbed equaled the amount of formic acid displaced. Similarly, when 8 μL of H_2O was injected, H_2O displaced formic acid in a 1 : 1.3 ratio. Another experiment repeated the adsorption procedure of Fig. 5, but TPD rather than PCO was carried out to determine if H_2O changes formic acid adsorption.Coadsorbing H_2O decreased formic acid coverage due to displacement, but it did not otherwise change the formic acid TPD spectra; all TPD products were detected at the same temperatures and the desorption curves had the same shapes with and without H_2O. Changing the order of adsorption (adsorbing H_2O before formic acid) did not change the resulting TPD spectra.

When 2 μL of H_2O was injected prior to PCO (Fig. 5), the normalized rate reached a maximum of 0.006 s^{-1}, remained fairly constant as PCO consumed approximately 10% of a formic acid monolayer, and then decreased throughout PCO. Quadrupling the amount of injected H_2O only displaced an additional 6% of a formic acid monolayer and the normalized rate reached the same maximum of 0.006 s^{-1}. However, the CO_2 formation rate started to decrease almost immediately after reaching a maximum. For all three experiments, the normalized rate was the same initially and it started to decrease at the same formic acid coverage. At longer reaction times, the normalized CO_2 formation rates were identical for PCO with and without coadsorbed H_2O.

PCO of ^{12}C- and ^{13}C-Formic Acid

Figure 6 shows PCO of a monolayer of ^{12}C-formic acid for 75 s, followed by an injection of 0.2 μL of ^{13}C-formic acid in the dark before the resumption of PCO. To minimize displacement of ^{12}C-formic acid, the amount of injected

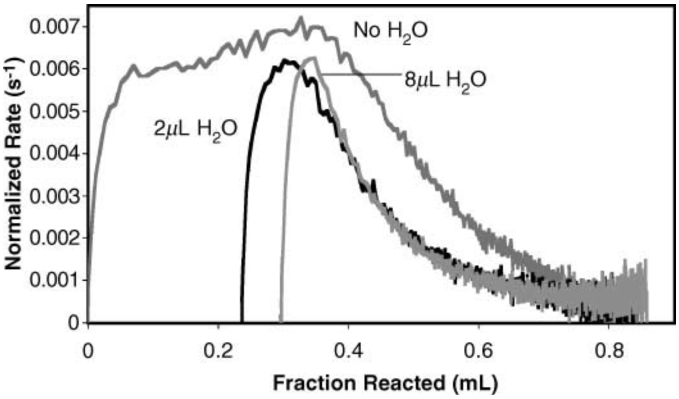

FIG. 5. Normalized CO_2 formation rates during room-temperature transient PCO of formic acid and coadsorbed H_2O/formic acid.

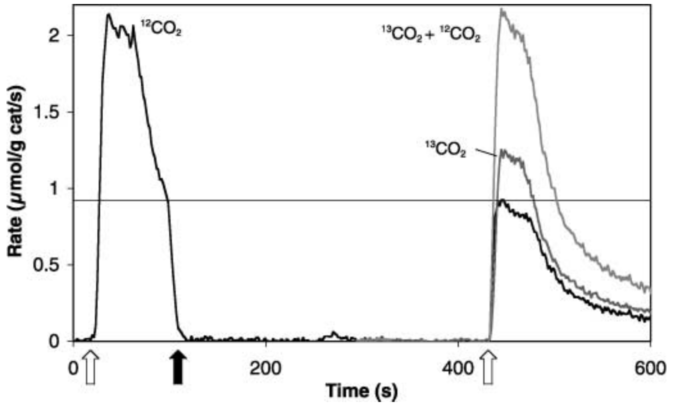

FIG. 6. CO_2 formation rates during transient PCO of formic acid. The UV lights were turned off (black arrow) at 100 s and ^{13}C-formic acid was injected in the dark before PCO resumed at 430 s (white arrow).

^{13}C-formic acid was an order of magnitude less than other pulses used in this study. Similar to Fig. 1, the $^{12}CO_2$ formation rate reached an immediate maximum, decreased slowly for approximately 30 s, and then dropped more quickly as PCO continued. After 75 s of UV irradiation, approximately 180 μmol/g catalyst of ^{12}C-formic acid oxidized to CO_2, leaving approximately 170 μmol/g catalyst adsorbed. After the UV lights were turned off, injecting ^{13}C-formic acid in the dark resupplied the sites left vacant by PCO; mass balances showed that approximately 170 μmol/g catalyst of ^{13}C-formic acid adsorbed. When the UV lights were turned back on at 430 s, the sum of the $^{12}CO_2$ and $^{13}CO_2$ formation rates was equal to the initial $^{12}CO_2$ formation rate, which indicates that catalyst activity after the dark time was the same as that initially. Figure 6 shows that the $^{12}CO_2$ formation rate was the same before and after the lights were turned off but that after the dark time it decreased more slowly than before for approximately 30 s and then decreased rapidly. The $^{13}CO_2$ formation rate also quickly reached a maximum, decreased slowly for 30 s, and subsequently dropped rapidly. Note that after adsorbing ^{13}C-formic acid, the $^{13}CO_2$ formation rate was 1.35 times that of the $^{12}CO_2$ rate, even though ^{12}C- and ^{13}C-formic acid coverages were nearly the same.

DISCUSSION

Mass Transfer and Other Experimental Artifacts

The behavior of P-25 (Fig. 1) during transient PCO does not appear to be due to nonuniform UV irradiation of the P-25 surface. Repeat experiments for catalysts with average film thicknesses ranging from 1.5 to 5 μm produced the same results as in Fig. 1. In addition, a previous study (31) of acetaldehyde PCO on several TiO_2 catalysts showed that the normalized CO_2 formation rates on some catalysts were approximately constant with coverage, indicating that UV irradiation was essentially uniform. In this study, the same coating procedure was used, the TiO_2 films were approximately the same thickness, and the UV lights and reactor were fixed in the same positions as in the previous study.

Several experiments determined that the PCO rate data were free of mass transfer limitations. Adsorbing formic acid in the dark ensured that the rate of formic acid diffusion and adsorption to the surface did not affect the PCO rate. Since CO_2 adsorbs weakly to TiO_2 at room temperature, its appearance in the gas phase is reaction limited; when the UV lights were turned off during PCO, the CO_2 formation rate dropped quickly to zero, indicating that CO_2 desorption and diffusion are fast compared to the surface reaction rate. Since CO_2 formation is reaction limited and formic acid produces CO_2 without forming any long-lived intermediates, monitoring the CO_2 formation rate during transient PCO is a direct measurement of the surface reaction rate. Another experiment determined that O_2 diffusion to the surface did not limit transient PCO; when the UV lights were turned off and back on during PCO, the CO_2 formation rate after the dark time was the same as before the UV lights were turned off. If O_2 diffusion to the surface limited PCO, O_2 would have diffused to the surface in the dark and the CO_2 formation rate would have increased when the lights were turned back on. This experiment also indicates that surface diffusion of formic acid to active sites did not limit PCO rate because formic acid also would have diffused to active sites in the dark.

During transient PCO of a formic acid monolayer (Fig. 1, bottom panel), the normalized CO_2 formation rate decreased dramatically as formic acid coverage decreased. The sharp drop in the normalized CO_2 formation rate during PCO might be explained by surface diffusion of active surface oxygen species limiting the PCO rate at low formic acid coverage. Formic acid that is adsorbed near oxygen adsorption sites would react initially and then oxygen would surface diffuse to formic acid adsorbed at greater distances from the oxygen adsorption sites as PCO proceeds. However, when PCO was carried out at one-half the typical UV intensity, the CO_2 formation rate was 59% of that at full intensity, and the shapes of the normalized CO_2 formation rate curves were exactly the same. That is, after multiplying the normalized CO_2 formation rate at half UV intensity by 1.7, *the curves were coincident at all coverages*. If oxygen surface diffusion limits PCO at low formic acid coverages, the normalized rate should begin to decrease at a lower coverage during PCO at one-half UV intensity because decreasing UV intensity would slow the surface reaction rate but not the rate of oxygen surface diffusion. Because the normalized CO_2 formation rate curves have exactly the same shape for different UV intensities, surface diffusion of active oxygen species does not limit PCO rate. In addition, this experiment confirms that diffusion of reactants and products does not limit PCO rate.

Active Sites

If all formic acid adsorption sites were equally active, the normalized rate in Fig. 1 (bottom panel) would be constant throughout PCO. If at least two adsorption sites of differing activity were present, the normalized rate would decrease initially, as formic acid was consumed on the more active sites, and eventually reach a constant value when only formic acid adsorbed on less-active sites remained. However, Fig. 1 (bottom panel) shows that the normalized rate increased slightly during the initial stages of PCO and reached a maximum after 35% of a formic acid monolayer formed CO_2. The initial increase in the normalized rate is attributed to H_2O, which formed during PCO and redistributed adsorbed formic acid. The normalized rate increased initially because formic acid displacement resupplied the more-active sites and the CO_2 formation rate was normalized by dividing it by the *total* formic acid coverage at each point in time. Further evidence of H_2O displacing adsorbed formic acid will be discussed in the following. When nearly all of the formic acid that is easily displaced by H_2O was removed, the normalized rate decreased and eventually reached a constant value, which is consistent with two types of active sites. At low formic acid coverage, the normalized rate was more than an order of magnitude less than the initial rate. At long reaction times, only formic acid on the less-active sites remained and therefore the normalized rate decreased at the same rate as coverage, producing a constant normalized rate (Fig. 1, bottom panel).

The variation in site activity may be due to differences in formic acid adsorption, but TPD was not sensitive enough to determine different forms of adsorbed formic acid. Popova *et al.* (32) used FTIR spectroscopy to study formic acid adsorption on anatase TiO_2. They determined that formic acid adsorbs both molecularly and dissociatively, in agreement with Liao *et al.* (33). In addition, they identified two types of dissociative adsorption: unsymmetrical and bidentate formate. These spectroscopy studies indicate that TiO_2 adsorbs formic acid molecularly and dissociatively at two formate adsorption sites. The primary role of weakly bound, molecularly adsorbed formic acid appears to be to resupply the formate adsorption sites, which are active for PCO. The two forms of adsorbed formate react at significantly different rates. These two formate adsorption sites will be hereafter referred to as the active sites and their activities will be discussed in the following.

Figure 6 also shows that at least two types of active sites exist for formic acid PCO. When ^{13}C-formic acid was adsorbed after 130 s of PCO of ^{12}C-formic acid, the $^{13}CO_2$ formation rate was approximately 35% greater than that of $^{12}CO_2$, even though the coverages of ^{12}C- and ^{13}C-formic acid were approximately the same. This indicates that ^{13}C-formic acid preferentially adsorbed on more-active sites that were left vacant after the 130 s of PCO prior to ^{13}C-formic acid injection. In addition, the total CO_2 formation rate after ^{13}C-formic acid injection was the same as that initially, indicating that the drop in CO_2 formation rate during PCO is not due to deactivation.

The identification of two active sites for carboxylic acid PCO explains differences between steady-state and transient PCO studies. For example, previous steady-state studies (26, 27) of benzene and toluene PCO proposed that benzoic acid accumulates on the surface and poisons sites, whereas transient PCO studies (21, 24) found benzoic acid to react readily. Similarly, accumulation of formic and acetic acids has been proposed to block adsorption sites at steady state (28, 29), whereas transient PCO showed that both acids react quickly to CO_2 (4, 12–14). The initial rates during transient PCO primarily measure the activity of the sites that are more active during PCO. In contrast, steady-state studies identified carboxylic acids on the surface after PCO, which is presumably due to carboxylic acids adsorbed on less-active sites. That is, carboxylic acids react readily on the more-active sites and produce high reaction rates in transient studies. After steady-state PCO, however, carboxylic acids adsorbed on less-active sites are expected to be present on the surface since they react slowly on these sites and are more strongly bound than the original reactants (which were aromatics and alcohols in these studies). Therefore, carboxylic acids are expected to be on the surface during PCO regardless as to whether or not they poison the catalyst.

Effect of H_2O during Transient PCO

Understanding the role of H_2O is important since it forms and remains adsorbed during transient PCO of formic acid. Photocatalytic oxidations with coadsorbed H_2O and formic acid (Fig. 5) clearly showed that H_2O displaced adsorbed formic acid. Muggli *et al.* (3) determined that approximately 750 μmol H_2O/g catalyst adsorbed on P-25 at room temperature. After an injection of 2 μL of H_2O, which corresponds to approximately 5 monolayer equivalents of H_2O, only 90 μmol/g catalyst H_2O adsorbed, which is 12% of an H_2O monolayer. Each adsorbed molecule of H_2O displaced one molecule of formic acid so that approximately three-fourths of a formic acid monolayer remained adsorbed. When the amount of injected H_2O quadrupled to approximately 20 monolayer equivalents, H_2O displaced formic acid in a 1 : 1.3 ratio. Quadrupling the amount of pulsed H_2O only displaced 20% more formic acid. That is, injecting 20 monolayer equivalents of H_2O displaced only 110 μmol formic acid/g catalyst, which is approximately 30% of the adsorbed formic acid monolayer. This suggests that H_2O readily displaces approximately one-third of a formic acid monolayer but competes less effectively for the sites to which the remaining formic acid adsorbed. Weakly bound formic acid that is easily displaced by H_2O is most likely molecularly adsorbed, as indicated by Liao *et al.* (33). They studied formic acid adsorption with FTIR and reported that 30% of the adsorbed formic acid was molecularly adsorbed and the remaining 70% adsorbed dissociatively as formate.

As discussed previously, the increasing normalized CO_2 formation rate during the initial stages of PCO (Fig. 1, bottom panel) was attributed to H_2O displacing formic acid, which replenished the more-active sites. When most of the formic acid that is easily displaced by H_2O was removed, the normalized CO_2 formation rate decreased quickly since the more-active PCO sites were not being resupplied with formic acid as readily as before. Coadsorbed H_2O/formic acid PCOs (Fig. 5) also show that injecting H_2O removed formic acid that is easily displaced so that the normalized rate started to decrease at the same coverage as did a formic acid monolayer. These results are also similar to those of Figs. 2 and 3, where heating removed a portion of adsorbed formic acid. That is, when formic acid coverage was approximately 65% of a monolayer, the normalized rate started to decrease regardless of whether the means used to reduce coverage was PCO (Fig. 1, bottom panel), H_2O injections (Fig. 5), or heating (Figs. 2 and 3).

In contrast to the coadsorbed H_2O/formic acid experiments, when H_2O was pulsed into the reactor after 300 s of transient PCO of formic acid, the CO_2 formation rate increased fourfold. This also appears to be due to H_2O displacing formic acid. When H_2O was pulsed into the reactor during PCO, formic acid that remained on the surface was adsorbed primarily on less-active sites since formic acid on more-active sites already reacted. The H_2O pulse displaced formic acid, which presumably readsorbed on the vacant more-active sites and thus increased the CO_2 formation rate. A similar experiment was performed in which formic acid PCO was stopped after 80 s and H_2O was injected in the dark; when PCO resumed, the CO_2 formation rate had approximately doubled. In both experiments, injecting H_2O apparently redistributed formic acid. At the time of H_2O injection, formic acid coverage on the more-active sites was low whereas coverage on less-active sites was high due to the large differences in activity. Therefore, since H_2O redistributed formic acid on the surface, the net effect of H_2O was to transport formic acid from less-active to more-active sites. These results are similar to those shown in Fig. 4, where heating the catalyst to 373 K in the dark redistributed adsorbed formic acid. That is, plots of normalized rates versus fraction of formic acid that reacted were nearly identical for PCO interrupted by either heating or injecting H_2O in the dark. This indicates that injecting H_2O produced the same effect as heating to 373 K; formic acid was redistributed on the surface. Another experiment repeated the procedure of that shown in Fig. 4 but a 0.2-μL pulse of H_2O, injected after heating the catalyst to 373 K and cooling to room temperature in the dark, replenished the surface with H_2O after heating removed some of the adsorbed H_2O. When PCO resumed, the CO_2 formation rate was nearly the same as that after the first dark period in Fig. 4, indicating that the increase in PCO rate in Fig. 4 was not due to the removal of adsorbed H_2O.

Figure 6 also suggests that H_2O, produced during PCO of formic acid, displaced adsorbed formic acid to more-active sites. After PCO of ^{12}C-formic acid and injection of ^{13}C-formic acid in the dark, the $^{12}CO_2$ formation rate was the same before and after the dark period, indicating that injecting ^{13}C-formic acid did not displace ^{12}C-formic acid. Even though the ^{12}C-formic acid was adsorbed on the same sites, *the $^{12}CO_2$ formation rate decreased more slowly when PCO resumed than before the dark period*. Adsorbing ^{13}C-formic acid increased formic acid coverage and therefore increased the rate that PCO produced H_2O, which displaced ^{12}C-formic acid from less-active to more-active sites.

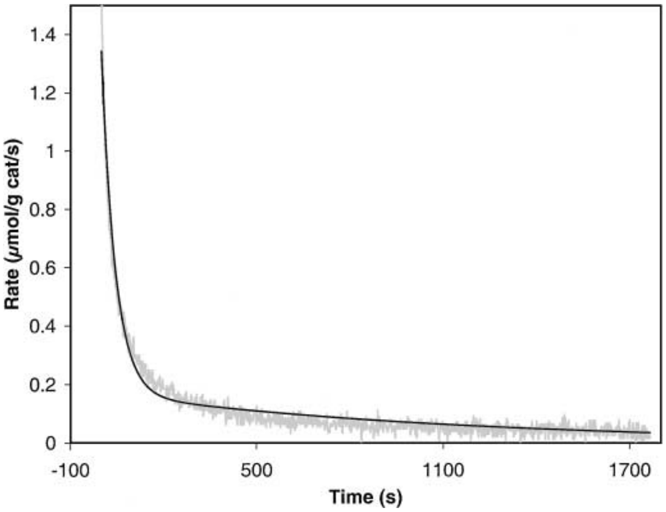

FIG. 7. Decay curve for CO_2 formation with two-site model fit.

Two-Site Model

Figure 1 (bottom panel) showed that during transient PCO of a formic acid monolayer, the normalized rate increased initially. As discussed previously, this increase is most likely due to displacement of weakly bound formic acid by H_2O. After 35% of a formic acid monolayer formed CO_2, the normalized rate decreased quickly, apparently because most of the weakly bound formic acid had been displaced by H_2O. This portion of the normalized CO_2 formation rate was fit to a two-site model (Fig. 7) to estimate the number and activity of less- and more-active sites. The following two-site model assumes constant oxygen concentration and therefore first-order surface reactions:

$$\mathrm{HCOOH}_{(\mathrm{site\,1})} \overset{k_1}{\Rightarrow} CO_2 + H_2O$$
$$\mathrm{HCOOH}_{(\mathrm{site\,2})} \overset{k_2}{\Rightarrow} CO_2 + H_2O.$$

Because mass balances determine the total formic acid coverage, the model contains three adjustable parameters: k_1, k_2, and the ratio of formic acid coverage on sites 1 and 2. The value determined for k_1 ($2 \times 10^{-2}\ \mathrm{s}^{-1}$) was approximately 20 times that of k_2 ($9 \times 10^{-4}\ \mathrm{s}^{-1}$), indicating a substantial difference in site activities. This model predicts that the more-active sites comprise approximately one-fourth of the total number of formic acid adsorption sites. The predicted coverage assumes that when the normalized CO_2 formation rate started to decrease in Fig. 1 (bottom panel), the formic acid coverage on the more-active sites was approximately 90%. This estimate was based on the large difference in site activities predicted by this model and a CO_2 formation rate that was 90% of the initial rate.

As mentioned previously, H_2O displaces formic acid, which mainly occurs during the initial stages of reaction. To obtain the simplest model that adequately fits the data, the model used here does not include this displacement, which is less important at lower coverages. Since H_2O

displacement redistributes formic acid on the surface, which in effect transports formic acid from high coverage regions (less-active sites) to low coverage regions (more-active sites), this model overestimates site 1 coverage and underestimates both site 2 coverage and the difference in site activities. Thus the values reported here represent lower limits for site 1 activity and site 2 coverage and upper limits on site 1 coverage and site 2 activity.

Effect of Heating

Heating TiO_2 from room temperature to 373 K (Fig. 3) dramatically increased PCO activity; although formic acid coverage at 373 K was 85% of that at room temperature, the initial CO_2 formation rate doubled. At longer reaction times, the effect of heating was more dramatic. For example, when one-fourth of a formic acid monolayer remained adsorbed, the normalized CO_2 formation rate at 373 K was eight times that at room temperature. This may indicate that formic acid oxidation is activated and the activation energy of the less-active sites is greater than that of the more-active sites, or formic acid adsorbed at less-active sites is more readily transported to more-active sites at 373 K. Onishi *et al.* (34) studied formic acid decomposition on TiO_2. They observed that when part of a formic acid monolayer was removed at 350 K, an ordered (2×1) formic acid adsorption structure could not be maintained due to surface diffusion. They proposed that formic acid may surface diffuse above 350 K and noted that the melting point of TiHCOO was only 374 K. However, in an experiment in which the UV lights were turned off for 1800 s and then back on after 180 s of transient PCO at 373 K (data not shown), the CO_2 formation rate was the same before and after the dark period. If the increase in the PCO rate at 373 K was due to faster formic acid surface diffusion, formic acid would have diffused to more active sites in the dark and therefore the CO_2 formation rate would have increased when PCO resumed. Therefore, formic acid surface diffusion does not appear to affect the formic acid PCO rate at temperatures between 273 and 373 K.

Although Fig. 3 shows that increasing temperature decreased the initial formic acid coverage, the normalized rate started to decrease at about the same coverage for all reaction temperatures. As mentioned previously, the normalized CO_2 formation rate decreased due to depletion of formic acid that is easily displaced by H_2O. Because the normalized rates decreased at the same coverages for each PCO temperature, the formic acid that was removed by heating in Fig. 3 appears to be the same formic acid that is easily displaced by H_2O. Similarly, Fig. 2 shows that heating to 373 K prior to room-temperature PCO removed a portion of the weakly bound formic acid and the normalized CO_2 formation rate started to decreased at the same coverage as that of PCO of a formic acid monolayer.

CONCLUSIONS

During PCO on TiO_2, formic acid oxidizes to CO_2 in a single step without forming long-lived intermediates. Less than one-fourth of the formic acid adsorption sites are highly active for PCO; these sites are at least 20 times more active than other formic acid adsorption sites. Water readily displaces approximately one-third of a formic acid monolayer whereas it does not effectively compete for adsorption sites with the remaining formic acid. Mass balances showed that, on average, each adsorbed H_2O molecule displaces one formic acid molecule. Water that is produced during PCO redistributes adsorbed formic acid on the surface by displacement. During transient PCO, redistributing surface coverage transports formic acid from less-active to more-active sites, which enhances the formic acid oxidation rate. Adsorbed H_2O does not poison the PCO activity of TiO_2. Heating TiO_2 to 373 K also redistributes adsorbed formic acid and the maximum CO_2 formation rate during PCO at 373 K was twice that at room temperature.

ACKNOWLEDGMENT

Acknowledgment is made to the Donors of the Petroleum Research Fund, administered by the American Chemical Society, for support of this research.

REFERENCES

1. Nimlos, M. R., Wolfrum, E. J., Brewer, M. L., Fennell, J. A., and Bintner, G., *Environ. Sci. Technol.* **30**, 3102 (1996).
2. Muggli, D. S., Larson, S. A., and Falconer, J. L., *J. Phys. Chem.* **100**, 15886 (1996).
3. Muggli, D. S., Lowery, K. H., and Falconer, J. L., *J. Catal.* **180**, 111 (1998).
4. Muggli, D. S., McCue, J. T., and Falconer, J. L., *J. Catal.* **173**, 470 (1998).
5. Jacoby, W. A., Blake, D. M., Fennell, J. A., Boulter, J. E., Vargo, L. M., George, M. C., and Dolberg, S. K., *J. Air Waste Manage. Assoc.* **46**, 891 (1996).
6. Sauer, M.-L., and Ollis, D.-F., *J. Catal.* **149**, 81 (1994).
7. Vorontsov, A. V., Barannik, G. B., Snegurenko, O. I., Savinov, E. N., and Parmon, V. N., *Kinet. Catal.* **38**, 84 (1997).
8. Peral, J., and Ollis, D.-F., *J. Catal.* **136**, 554 (1992).
9. Cunningham, J., Hodnett, B. K., and Walker, A., *Proc. R. Irish Acad.* **77B**, 411 (1977).
10. Kennedy, J. C., and Datye, A. K., *J. Catal.* **179**, 375 (1998).
11. Muggli, D. S., and Falconer, J. L., *J. Catal.* **175**, 213 (1998).
12. Muggli, D. S., and Falconer, J. L., *J. Catal.* **187**, 230 (1999).
13. Muggli, D. S., and Falconer, J. L., *J. Catal.* **191**, 318 (2000).
14. Muggli, D. S., Keyser, S. A., and Falconer, J. L., *Catal. Lett.* **55**, 129 (1998).
15. Muggli, D. S., and Falconer, J. L., *J. Catal.* **181**, 155 (1999).
16. Jacoby, W. A., Nimlos, M. R., and Blake, D. M., *Environ. Sci. Technol.* **28**, 1661 (1994).
17. Blount, M. C., Kim, D. H., and Falconer, J. L., *Environ. Sci. Technol.* **35**, 2988 (2001).
18. Muggli, D. S., and Ding, L. F., *Appl. Catal. B: Environ.* **32**, 181 (2001).
19. Lee, G. D., and Falconer, J. L., *Catal. Lett.* **70**, 145 (2000).
20. Lee, G. D., Tuan, V. A., and Falconer, J. L., *Environ. Sci. Technol.* **35**, 1252 (2001).
21. Blount, M. C., and Falconer, J. L., *J. Catal.* **200**, 21 (2001).

22. Blount, M. C., Buchholz, J. A., and Falconer, J. L., *J. Catal.* **197**, 303 (2001).
23. Larson, S. A., and Falconer, J. L., *Appl. Catal. B: Environ.* **4**, 325 (1994).
24. Larson, S. A., and Falconer, J. L., *Catal. Lett.* **44**, 57 (1997).
25. Larson, S. A., Widegren, J. A., and Falconer, J. L., *J. Catal.* **157**, 611 (1995).
26. Cao, L. X., Gao, Z., Suib, S. L., Obee, T. N., Hay, S. O., and Freihaut, J. D., *J. Catal.* **196**, 253 (2000).
27. Mendez-Roman, R., and Cardona-Martinez, N., *Catal. Today* **40**, 353 (1998).
28. Sauer, M. L., and Ollis, D. F., *J. Catal.* **158**, 570 (1996).
29. Obuchi, E., Sakamoto, T., Nakano, K., and Shiraishi, F., *Chem. Eng. Sci.* **54**, 1525 (1999).
30. Kozlov, D. V., Paukshtis, E. A., and Savinov, E. N., *Appl. Catal. B: Environ.* **24**, L7 (2000).
31. Muggli, D. S., Ding, L., and Odland, M. J., *Catal. Lett.* **78**, 23 (2002).
32. Popova, G. Y., Andrushkevich, T. V., Chesalov, Y. A., and Stoyanov, E. S., *Kinet. Catal.* **41**, 805 (2000).
33. Liao, L. F., Wu, W. C., Chen, C. Y., and Lin, J. L., *J. Phys. Chem. B* **105**, 7678 (2001).
34. Onishi, H., Aruga, T., and Iwasawa, Y., *J. Catal.* **146**, 557 (1994).